A Mesoscopic Human-Inspired Adaptive Cruise Control for Eco-Driving

Marco Mirabilio, Alessio Iovine, Elena De Santis, Maria Domenica Di Benedetto, Giordano Pola

A Mesoscopic Human-Inspired Adaptive Cruise Control for Eco-Driving

Marco Mirabilio, *Student Member, IEEE*, Alessio Iovine, *Member, IEEE*, Elena De Santis, *Senior Member, IEEE*, Maria Domenica Di Benedetto, *Fellow, IEEE*, Giordano Pola, *Senior Member, IEEE*

***Abstract*—Interconnected and autonomous vehicles are proven to be helpful in reducing traffic congestion and dangerous emissions while enhancing safety on our roads. In this context, the present paper introduces a human-inspired Adaptive Cruise Control dedicated to improving the passenger experience using Model Predictive Control and traffic macroscopic information. To better describe the characteristics of human drivers, first a human-inspired microscopic hybrid automaton is considered, and an optimization problem targeting consumption minimization and collision avoidance is designed with a receding horizon approach. Then, traffic macroscopic information is included in the controller definition so that a mesoscopic Adaptive Cruise Control model is obtained. Simulations showing the efficacy of the proposed approaches for safety and eco-driving are provided.**

***Index Terms*—Interconnected and Autonomous Vehicles, Adaptive Cruise Control (ACC), Hybrid Automaton, Mesoscopic Model, Eco-Driving, Model Predictive Control (MPC)**

I. Introduction

Interconnected and autonomous vehicles are expected to have large diffusion in the next future. Indeed, they offer the possibility of employing complex control strategies for traffic flow efficiency improvement, thus reducing traffic jamming, consumption and car accidents [1], [2], [3], [4]. To this purpose, different vehicular communication systems have been proposed in the current literature, based on the Dedicated Short Range Communication technology (DSRC) and generally grouped in the Vehicle-to-Everything family (V2X) [5], [6], [7]. Recently, with the goal of improving passenger comfort and vehicle responsiveness to the external environment, the capability of self-driving cars to imitate human behavior has gained importance in the controllers definition. This new goal requires rethinking the controllers' design process in a way that considers human characteristics in the development of novel autonomous driving strategies [8], [9]. The present paper contributes to this research line by suggesting a human-inspired Adaptive Cruise Control (ACC) for autonomous vehicles, which ensures collision avoidance while maximizing comfort and minimizing fuel consumption. To this goal, the ACC is designed to mimic the human driver behavior when different situations are encountered (e.g., free run and danger), similarly to [10] and [11]. Differently, the ACC implements optimal control strategies via Model Predictive Control (MPC), but also adapts its perceptions and predictions with respect to the traffic flow seen from a macroscopic perspective. The developed controller, which is capable of mixing microscopic (leader-follower interactions) and macroscopic (traffic flow) information, is therefore named mesoscopic. With respect to classical microscopic controllers, based only on local leader-follower information, the mesoscopic ones improve vehicles responsiveness, especially in convoluted scenarios and during transients. Philosophically, they are similar to a smart human driver that adapts the driving style to current traffic state. Moreover, they are capable to ensure String Stability without using any information of the first vehicle of the platoon [12], [13], [14].

Classically, the family of micro-macro or mesoscopic models are derived by introducing microscopic information in a macroscopic framework, with the aim of studying the effect of flow management strategies locally on each vehicle (e.g., on the consumption [15]). On the contrary, in the present paper, macroscopic information is used in the local controller in a bottom-up approach. The possibility to use macroscopic information in a microscopic framework is not novel in the literature. For example, other approaches based on the idea of using macroscopic information for local control purposes can be found in [12], [13], [14], [16], [17] and [18]. In [16], the authors propose a control strategy that considers traffic density data, and the classic conservation of mass equation described by a Partial Differential Equation (PDE). Then, they perform a theoretical stability analysis by means of linearization techniques around some equilibrium point. The focus is merely on traffic stability, while no consumption minimization goals and formal safety guarantees are considered. In [17], the management of a congested traffic situation is considered. Due to the presence of a bottleneck ahead, the authors define a variable to be computed by the platoon leader vehicle to catch the existence of a shock-wave and its propagating velocity. Then, this variable is exploited within an MPC framework to appropriately adapt the speed of the cluster, thus anticipating the slow-down maneuver. In [12] and [14], the authors focus on the String Stability problem for a platoon where each vehicle's controller exploits macroscopic information in the nominal case and in the case of vehicles subject to external disturbances, respectively. Then, the possibility to ensure String Stability for a class of mesoscopic models described by Ordinary Differential Equations (ODEs) is proven, thus ensuring that the perturbations arising in the platoon do not amplify through it. However, no formal safety analysis is

Marco Mirabilio, Elena De Santis, Maria Domenica Di Benedetto and Giordano Pola are with the Department of Information Engineering, Computer Science and Mathematics, Center of Excellence DEWS, University of L'Aquila. (e-mail: marco.mirabilio@graduate.univaq.it, {elena.desantis,mariadomenica.dibenedetto,giordano.pola}@univaq.it)

Alessio Iovine is with the CNRS and Laboratoire des Signaux et Systèmes (L2S), CentraleSupélec, Université Paris-Saclay, 3, rue Joliot-Curie, 91192 Gif-sur-Yvette, France. E-mail: alessio.iovine@centralesupelec.fr

performed, and no optimal control problem for eco-driving is defined. Similarly, String Stability by exploiting macroscopic information related to the fundamental diagram is investigated in [13]. In [18], the platoon is seen as an intelligent actuator that can improve traffic efficiency. The interaction between the bulk traffic flow and the platoon of connected vehicles are described with a coupled PDE-ODE. Then, the speed trajectories of the leading vehicle and of the last one are optimized via a MPC algorithm. Differently from [18], in the present paper we define a variance-based mechanism for the control law of each vehicle to adapt to the current traffic situation.

We consider a platoon of homogeneous self-driving cars moving on a single lane highway (see Fig. 1). The modeling suggested in the present paper is inspired by [10] and [11] where a hybrid automaton is defined (see [19], [20]), and, differently from here, only collision avoidance is guaranteed and no implementation of optimal strategies or eco-driving goal is targeted. Specifically, the discrete states of the hybrid automaton are used to describe the psycho-physical perception of the risk that is felt by humans while driving, on the basis of the Wiedemann and Fritsche's models of [21] and [22], respectively. Consequently, each discrete state is associated with a different car-following situation, and the controller behavior is adapted while switching among them as a human being would do. For example, a dangerous situation requires reactive responses where passengers' comfort is not considered. On the contrary, a safe situation allows for smoother behavior that focuses on a trade-off between performance and passengers' pleasure.

A different control law is associated to each car-following situation desribed by the discrete states of the human-inspired hybrid automaton. In [10] and [11], stimulus-response control laws ensure collision avoidance, i.e., safety. Differently, the use of MPC allows to consider the optimal speed and acceleration trajectories while ensuring collision avoidance and consumption reduction, commonly named eco-driving [23], [24], [25], [26], [27], [28]. Therefore, in the present paper, an MPC-based optimization problem is defined, where a different cost function is considered for each discrete state of the hybrid automaton, according to the specific trade-off among the goals of each discrete state. Preliminary results on the utilisation of MPC strategies for the proposed hybrid automaton are suggested in [29], where a computational demanding exponential function for the fuel consumption computation is employed to pursue the eco-driving goal. Here, we adopt the polynomial function introduced in [18] and [30] for estimating the fuel consumption, thereby obtaining a lower computational burden with respect to the exponential function in [29]. Moreover, a more detailed computation of the admissible regions of the state space is provided here. Also, no macroscopic information is considered in [29], thus providing only a microscopic controller. On the contrary, the present paper suggests also a variance-based mechanism exploiting macroscopic variables, with the purpose of providing a mesoscopic controller and improving its response. Therefore, we develop a human-inspired MPC-based ACC for autonomous vehicles that targets both consumption minimization and collision avoidance and, in order to improve the single vehicle controller response, exploits the information contained in the macroscopic variables describing the traffic state. Simulations of platoons implementing both the controller based only on local information (microscopic controller) and the one exploiting also macroscopic information (mesoscopic controller) have been performed in order to compare the two control strategies.

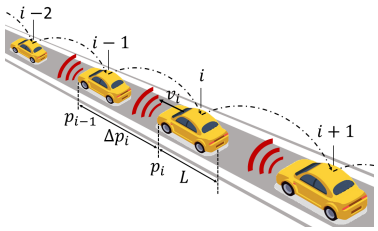

Fig. 1: Single lane highway reference framework. The dash-dot arrows represent the information flow propagation.

Each vehicle is supposed to correctly measure the distance and speed of its predecessor by means of appropriate sensors. Moreover, vehicles are assumed to interconnect with the surrounding agents, either via Vehicle-to-Vehicle (V2V) or Vehicle-to-Infrastructure (V2I) technologies, or both. As in [31] and [32], each vehicle is sending information about the predicted trajectory evolution to its follower, yielding a distributed receding horizon controller. The global traffic state information is shared using only a few variables, thus reducing the communication burden and avoiding the need for more complex information flow topology, as for example the "Predecessor Following Leader" or the "Bidirectional Leader" (see [33] and [34]). The proposed control approaches are then tested in two different information scenarios: i) the vehicles in the platoon consider only the trajectory forecast of each leading vehicle shared through a dedicated inter-vehicular message. The microscopic MPC is implemented, resulting in a microscopic closed-loop model; ii) the vehicles exploit the trajectory forecast sent by the vehicle ahead and the traffic macroscopic information. This leads to a mesoscopic controller and a mesoscopic closed-loop model. The provided simulations show that the string of vehicles is always able to ensure collision avoidance. Moreover, they illustrate how the introduction of the macroscopic information in the control strategy is able to improve the overall platoon behaviour with respect to perturbations deriving from unexpected speed variations.

The rest of the paper is organized as follows: in Section II we introduce the platoon modeling and discuss the problem formulation; in Section III we define the microscopic optimal control problem; in Section IV we introduce the use of macroscopic information, and how it modifies the before mentioned modeling; Section V provides simulations results; Section VI reports some conclusive remarks.

II. Platoon Modeling and Problem Formulation

We consider a set of $N+1$ equal autonomous vehicles moving on a highway (see Fig. 1), $N \in \mathbb{N}$, where $i=0$ is the first vehicle and $\mathcal{I}_N = \{1, ..., N\}$ is the set of followers. The overall set of vehicles is denoted by $\mathcal{I}_N^0 = \{0\} \cup \mathcal{I}_N$. Then,

two major cases are modeled: a *free running* situation, with no vehicles ahead, and a *car-following* situation. Vehicles are assumed to be interconnected, and to send/receive data to/from the surrounding environment, either via V2V or V2I technologies, or both. Regardless of the communication technology adopted, we assume a unidirectional information flow as in Fig. 1. We stress that we do not consider direct communication between the platoon leading vehicle and the others in case of platoons composed by more than two vehicles, or more complex communication topologies, as generally granted in cooperative platoons [33], [34].

A. Platoon model

We consider a dynamical model based on the elementary equations describing the longitudinal motion of a vehicle (see [35, Chapter 2]). Since our objective is to implement a MPC-based controller, we consider a discrete time system. As in [32], we assume the vehicles to move on a flat and dry road, we neglect the tire slip in the longitudinal direction, and we do not model the aerodynamic drag reduction phenomenon when two, or more, vehicles follow each other. We define $\tau \in \mathbb{R}^+$ as the sampling time and $k\tau$, $k \in \mathbb{N}$, as the k-th sampling time. Given the i-th vehicle, $i \in \mathcal{I}_N^0$, its longitudinal position and velocity are denoted by $p_i(k) \geq 0$ and $0 \leq v_i(k) \leq v_{\max}$, respectively, with dynamics

$$\begin{aligned} p_i(k+1) &= p_i(k) + v_i(k)\tau \\ v_i(k+1) &= v_i(k) + \tfrac{\tau}{m_v}\Big(F_{T,i}(k) - F_{res}(v_i(k))\Big) \end{aligned}, \quad (1)$$

where m_v is the vehicle mass; $F_{T,i} \in [F_{T,\min}, F_{T,\max}]$ is the traction force assumed operating as the control input, $F_{T,\min} < 0 < F_{T,\max}$; the resistance force acting on the vehicle is $F_{res}(v_i(k)) = F_a(v_i(k)) + F_r$, with $F_a(v_i(k)) = c_{aero}v_i(k)^2$ the aerodynamic drag force, $c_{aero} > 0$ the coefficient of aerodynamic drag, $F_r = c_{roll}gm_v$ the rolling resistance, $c_{roll} > 0$ the rolling friction coefficient; g is the gravity acceleration. Since we assume $v_i(k) \in [0, v_{\max}]$, then $0 \leq F_a(v_i(k)) \leq c_{aero}v_{\max}^2$. As a consequence, the resistance force is bounded between $F_{res,\min} = c_{roll}gm_v$ and $F_{res,\max} = c_{roll}gm_v + c_{aero}v_{\max}^2$. As in [32] and [36], we assume that the box constraints on the traction force can be reflected by desired values of maximum acceleration and deceleration, i.e., $a_{\max} > 0$ and $a_{\min} < 0$ respectively. From (1), we derive the dynamic model describing the interactions in the i-th leader-follower pair $(i-1, i)$ with respect to the follower point of view. Let us define the state vector x_i as

$$x_i = \left[\ \Delta p_i\ \ \Delta v_i\ \ v_{i-1}\ \right]^T, \quad (2)$$

where $\Delta p_i = p_{i-1} - p_i$, $\Delta v_i = v_{i-1} - v_i$, and v_{i-1} is the speed of the preceding vehicle. Then, the dynamical model associated to (2) is

$$\begin{aligned} x_i(k+1) = Ax_i(k) + B_u u_i(k) \\ + B_d a_{i-1}(k) + E a_{res}(x_i(k)), \end{aligned} \quad (3)$$

where $u_i = F_{T,i}/m_v$, $a_{res}(x_i) = F_{res}(x_i)/m_v$, and $a_{i-1} \in [a_{\min}, a_{\max}]$ is the point-mass acceleration of the preceding vehicle (here seen as a bounded disturbance), and

$$A = \begin{bmatrix} 1 & \tau & 0 \\ 0 & 1 & 0 \\ 0 & 0 & 1 \end{bmatrix},\ B_u = \begin{bmatrix} 0 \\ -\tau \\ 0 \end{bmatrix}, \quad (4)$$
$$B_d = [0\ ,\ \tau\ ,\ \tau]^T\ ,\ \ E = [0\ ,\ \tau\ ,\ 0]^T$$

As in [17], we assume the existence of a low level controller that receives the control input u_i computed by the controller as reference value, and manages the powertrain unit and its dynamics accordingly. Let a "collision" be defined as follows:

Definition 1. *A collision is the event corresponding to a bumper-to-bumper distance between two vehicles less than a margin $s > 0$, $s \in \mathbb{R}$.*

Then, we assume the following

Assumption 1. *All the vehicles share the goal of collision avoidance when in a car-following situation.*

For (3) to describe also the dynamics of the first vehicle of the platoon, we assume the existence of a virtual leader indexed by $i = -1$, with constant speed v_{-1} corresponding to the desired speed $v^r \geq 0$ of $i = 0$. For the pair $(-1, 0)$, we set the fictitious distance $\Delta p_0(t) = \Delta\bar{p} >> s$, $\forall\, t \geq 0$.

Together with physical and legal limits, Definition 1 and the leader-follower state vector (2) lead to the following set $X \subseteq \mathbb{R}^3$ of admissible states for $x_i(k)$:

$$\begin{aligned} X = \{x_i \in \mathbb{R}^3 : \Delta p_i \geq s,\ -v_{\max} + v_{i-1} \leq \Delta v_i \leq v_{i-1}, \\ 0 \leq v_{i-1} \leq v_{\max}\}. \end{aligned} \quad (5)$$

Our aim is to compute the optimal control, among all the control laws that ensure safety, which minimizes a state-dependent cost function that takes into account emissions (eco-driving specifications) and errors with respect to the desired distance between two consecutive vehicles and the desired velocity. To this purpose, we assume that each vehicle knows the position, velocity, and acceleration of its predecessor.

B. Human Psycho-Physical Thresholds

Inspired by the models in [21], [22]), and according to the automaton in [29], to embed the human psycho-physical perception and responsiveness in the controller we partition the set X on the basis of the psycho-physical thresholds that separate the different psychological situations the driver feels. Then, each partition of X is associated with a discrete state of the hybrid automaton defined in Section II-C. To this goal, we define:

■ *Emergency Distance* $\Delta E : \mathbb{R}^3 \to \mathbb{R}$

It is the minimum distance ensuring collision avoidance in the worst case scenario, that is when the leader brakes with maximum deceleration until the full stop:

$$\Delta E(x_i) = s + \begin{cases} 0 & \Delta v_i > 0 \\ \frac{\Delta v_i^2}{2|a_{\min}|} - \frac{\Delta v_i v_{i-1}}{|a_{\min}|} & \Delta v_i \leq 0. \end{cases} \quad (6)$$

If at time k the distance is equal to $\Delta E(x_i(k))$ and the leader starts braking with the maximum deceleration, provided that

the follower also brakes at the same time with the maximum deceleration, then collision is avoided. In addition, we define functions $T_R : \mathbb{R}^3 \to \mathbb{R}$ and $T_S : \mathbb{R}^3 \to \mathbb{R}$ as

$$T_R(x_i) = \frac{v_{i-1} - \Delta v_i}{|a_{\min}|}, \; T_S(x_i) = \lambda T_R(x_i) \tag{7}$$

and the constant time $T_D > 0$, where:

- T_R, or risky time, is the time needed to stop the vehicle from speed $v_i = v_{i-1} - \Delta v_i$ with deceleration $a_{\min}$.
- T_S, or safety time, is the time needed to stop the vehicle from speed $v_i = v_{i-1} - \Delta v_i$ with a comfortable deceleration $a_{\min}/\lambda$, $\lambda > 1$.
- T_D, or interaction time, is the time headway beyond which the vehicle ahead can be ignored [11].

On the basis of the time headways in (7), we define the following additional thresholds for the distance Δp_i:

■ *Risky Distance* $\Delta R : \mathbb{R}^3 \to \mathbb{R}$

$$\Delta R(x_i) = \Delta E(x_i) + s_r(x_i) + c_r T_R(x_i) v_{i-1} \tag{8}$$

This distance takes into account the human time response, modeled by the term $c_r T_R(x_i) x_{i-1}$ that represents the additional space covered before the driver responds to the leader's actions, where $c_r > 0$ is a constant multiplicative factor. Depending on the environment information and human perception, such value can increase (more cautious behavior), or decrease (more aggressive behavior). Differently from [29], in order to avoid that ΔR collapses to ΔE when the vehicles are at a full stop, we add the term

$$s_r(x_i) = \frac{\tau^2}{2}(a_{\max} - a_{\min}) + \begin{cases} 0, & \Delta v_i > 0 \\ -\Delta v_i \tau, & \Delta v_i \leq 0 \end{cases} \tag{9}$$

that corresponds to the difference between the distance traveled by the leader braking with $a_{\min}$ in a time step and the distance traveled by the follower accelerating with $a_{\max}$ in the same time step. As a consequence, $\Delta R(x_i) > \Delta E(x_i)$, $\forall\, x_i \in \mathbb{R}^3$.

■ *Safety Distance* $\Delta S : \mathbb{R}^3 \to \mathbb{R}$

$$\Delta S(x_i) = \Delta E(x_i) + s_s + c_s T_s(x_i) v_{i-1} \tag{10}$$

It represents the distance at which the human driver feels safe and the vehicle can be stopped without braking with the maximum effort, always guaranteeing collision avoidance. In order to ensure $\Delta S(x_i) > \Delta R(x_i)$, $\forall\, x_i$, we set the constant multiplicative factor $c_s \geq c_r$ and the constant $s_s > 0$. As for the risky distance, the term s_s avoids that $\Delta S(x_i)$ collapses to $\Delta E(x_i)$ and $\Delta R(x_i)$ at full stop.

■ *Interaction Distance* $\Delta D : \mathbb{R}^3 \to \mathbb{R}$

$$\Delta D(x_i) = \begin{cases} \Delta S(x_i) & \Delta v_i > 0 \\ s + s_d + c_d T_D(x_i) v_i & \Delta v_i \leq 0 \end{cases} \tag{11}$$

It represents a distance at which the driver takes into account the presence of its predecessor. This distance is characterized by the fixed time headway T_D, and for $\Delta v_i > 0$ it corresponds to the Safety Distance $\Delta S(x_i)$. The coefficients are such that $c_d > 0$ and $s_d > 0$.

The above introduced thresholds are used to define the partitions Ω_j, $j = 1, 2, 3, 4, 5$, of X defined below. For simplicity, we denote $\Delta E_i = \Delta E(x_i)$, $\Delta R_i = \Delta R(x_i)$, $\Delta S_i = \Delta S(x_i)$ and $\Delta D_i = \Delta D(x_i)$. Then,

$$\begin{aligned} \Omega_1 = \Big\{ & x_i \in X \,:\, (\Delta v_i > \epsilon_\Omega) \wedge (\Delta p_i > \Delta S_i) \,\cup \\ & (\Delta v_i \leq 0) \wedge (\Delta p_i > m_i) \,\cup \\ & (0 < \Delta v_i \leq \epsilon_\Omega) \wedge (\Delta p_i > m_{0,i}) \Big\}, \end{aligned} \tag{12}$$

where $\epsilon_\Omega > 0$, $m_i = \max(\Delta D_i, \Delta S_i)$, and $m_{0,i} = \max(\Delta D_{0,i}, \Delta S_{0,i})$. Here, $\Delta D_{0,i}$ and $\Delta S_{0,i}$ correspond to the values of ΔD_i and ΔS_i, respectively, when $\Delta v_i = 0$. Ω_1 corresponds to the region where the i-th vehicle can run freely since there is no ahead vehicle, or it is too far away. The role of variables ϵ_Ω and $m_{0,i}$ is to avoid multiple oscillations between Ω_1 and other regions when x_i is in a neighborhood of the $\Delta v_i = 0$ axis.

For $j = 2$,

$$\begin{aligned} \Omega_2 = \Big\{ & x_i \in X \,:\, (\Delta v_i > \epsilon_\Omega) \wedge (\Delta R_i < \Delta p_i \leq \Delta S_i) \,\cup \\ & (\Delta v_i < 0) \wedge (\Delta S_i < \Delta p_i \leq \Delta D_i) \,\cup \\ & (0 < \Delta v_i \leq \epsilon_\Omega) \wedge (\Delta R_i < \Delta p_i \leq m_{0,i}) \Big\}, \end{aligned} \tag{13}$$

We remark that, although $\Delta S_i > \Delta R_i$ is always verified, the same inequality does not always hold for ΔD_i. As a consequence, when $\Delta S_i \geq \Delta D_i$, Ω_2 disappears for $\Delta v_i < 0$. For $j = 3$,

$$\Omega_3 = \Big\{ x_i \in X \,:\, (\Delta v_i < 0) \wedge (\Delta R_i < \Delta p_i \leq \Delta S_i \Big\}. \tag{14}$$

The sets Ω_2 and Ω_3 correspond to the case where the follower vehicle is closing to the vehicle ahead. In particular, in Ω_3 the distances are lower than in Ω_2, representing the approaching of an alert situation. We remark also that, in some circumstances, Ω_3 can be empty, meaning that there is no more a transition region between Ω_2 and the set

$$\Omega_4 = \Big\{ x_i \in X \,:\, \Delta E_i \leq \Delta p_i \leq \Delta R_i \Big\}. \tag{15}$$

This last region represents a critical situation, where the distances are too close to the emergency value ΔE_i. Finally, we define

$$\Omega = \bigcup_{j=1}^{4} \Omega_j \tag{16}$$

as the admissible set where the leader-follower state trajectory can lie, and

$$\Omega_5 = X \setminus \Omega \tag{17}$$

as the critical region (unsafe region) where safety is not ensured with respect to the worst case scenario of the leader braking with maximum effort. We recall that adding the term $s_r(x_i)$ in the definition of ΔR_i in (8) ensures that Ω_4 does not disappear when $v_{i-1} = 0$. Moreover, it avoids a direct transition of the continuous state x_i from $\Omega_1, \Omega_2, \Omega_3$ to region Ω_5. We recall also that regions Ω_j do not overlap each other, i.e., $\Omega_l \cap \Omega_j = \emptyset$, $l \neq j$.

Fig. 2 shows Ω in the bi-dimensional space $(\Delta v_i, \Delta p_i)$, where partitions Ω_j are obtained by setting a constant speed

$v_{i-1} = 18$ m/s. Figures 3 and 4 offer a three-dimensional view of regions Ω_j for $v_{i-1} = \{0, 6, 12, 18, 24, 30, 36\}$ m/s (refer to Fig. 2 for the color meaning). Finally, Fig. 5 shows a three-dimensional view of set Ω, where we observe its non-convexity. However, it is controlled invariant by construction; indeed, it is straightforward to verify that the control law $u_i = a_{\min}$ makes Ω invariant.

C. Microscopic Hybrid Automaton

In this section, the microscopic hybrid automaton used to model the human way of driving is introduced. It is defined on the basis of regions Ω_j, $j = 1, 2, 3, 4, 5$, and it is exploited to vary the controller response with respect to the current car-following situation, as a human-driver would do. We refer to it as to be *microscopic*, since for now the model refers only to the i-th leader-follower pair, without taking into account macroscopic information describing the state of the platoon, or of the whole traffic flow. The hybrid automaton associated with the i-th car-following pair, $i \in \mathcal{I}_N^0$, is defined by the following tuple (see [19]):

$$\mathcal{H} = \big(Q, X_{\mathcal{H}}, U, D, F, Init, Dom, \mathcal{E}\big) \tag{18}$$

where:

- $Q = \{q_j,\ j = 1, 2, 3, 4, 5\}$ is the set of discrete states (or modes), each one associated with a partition of X, and representing the corresponding car-following situation;
- $X_{\mathcal{H}} = \mathbb{R}^3$ is the continuous state space;
- $U = [u_{\min}, u_{\max}]$ is the input space, where $u_{\min} = F_{T,\min}$, $u_{\max} = F_{T,\max}$;
- $D = [a_{\min}, a_{\max}]$ is the disturbance space, here considered as the point-mass acceleration of the preceding vehicle;
- $F = \{f_q,\ q \in Q\}$, $f_q : X_{\mathcal{H}} \times U \times D \to X_{\mathcal{H}}$, is the set of vector fields describing the evolution of the continuous state with respect to the discrete state q. Since the car-following dynamics does not change with the discrete state, then $F = \{f\}$ is a singleton:

$$x(k+1) = f(x(k), u(k), d(k)),\ \ k \in \mathbb{N}, \tag{19}$$

  with f defined in (3) and (4), $x \in X_{\mathcal{H}}$, $u : \mathbb{N} \to U$ and $d : \mathbb{N} \to D$;
- $Init \subseteq Q \times \Omega \subseteq Q \times X_{\mathcal{H}}$ is the set of initial discrete and continuous states;
- $Dom : Q \to \{\Omega_j,\ j = 1, 2, 3, 4, 5\}$ is the domain map;
- $\mathcal{E} = Q \times Q$ is the set of edges. Since we can not predict the discrete state future evolution, we have to assume that it can switch in every $q \in Q$. Then, the set $\mathcal{E}$ is not a subset of $Q \times Q$, but coincide with it.

The hybrid automaton state associated with the i-th vehicles pair is

$$\xi_i(k) = (x_i(k), q_i(k)) \in X_{\mathcal{H}} \times Q. \tag{20}$$

Right below, we describe the meaning of the discrete states $q \in Q$ associated with the different car-following scenarios, and the corresponding control action:

1) *Free driving* $= q_1$, $Dom(q_1) = \Omega_1$: there is no leader vehicle, or it is too far away. Consequently, the i-th vehicle can freely track its reference speed v^r with no safety concerns. The control action depends on the desired speed and on the fuel consumption rate.
2) *Following* $= q_2$, $Dom(q_2) = \Omega_2$: the follower vehicle can not ignore the presence of the vehicle ahead, but the distance is such that there is no immediate danger. The control action still depends on the fuel consumption, but also on the relative speed Δv_i, other than Δp_i.
3) *Closing in* $= q_3$, $Dom(q_3) = \Omega_3$: the speed difference is large and the distance is not, so the follower has to decelerate to avoid collision. The control action mainly depends on Δv_i and Δp_i, while the fuel optimization objective has a lower weight.
4) *Danger* $= q_4$, $Dom(q_4) = \Omega_4$: the distance from the previous vehicle is close to the unsafe one, then the control action depends only on Δv_i and Δp_i.
5) *Unsafe* $= q_5$, $Dom(q_5) = \Omega_5$: collision cannot be avoided.

In the definition of state q_1, two consecutive vehicles are considered to be in a leader-follower situation if their distance does not exceed a predefined "contact distance" $\Delta_{\max} > 0$. As in [11], the $Init$ set is defined as

$$Init = \bigcup_{i=1}^{4} \{q_i\} \times \{Dom(q_i)\}, \tag{21}$$

where the unsafe domain is not included.

We recall that by definition of the space thresholds introduced in this section, a direct transition of the continuous state from $\Omega_1, \Omega_2, \Omega_3$ to the unsafe zone Ω_5 is not possible. Therefore, a direct transition from states q_1, q_2, q_3 to q_5 is avoided.

III. Control Design

The objective of the controller design is to consider the aforementioned human psycho-physical characteristics in the control action. To this purpose, the controller development is adapted to the different car-following situations seen in normal traffic while taking into account consumption optimization and safety constraints. In the sequel, the information related to the different driving situations is translated in the MPC framework by appropriately varying the weights given to the control objectives, such fuel consumption or tracking of a desired distance. As a result, different cost functions for the discrete states are defined, each one focusing on a different trade-off among the desired goals.

A. Fuel Consumption Model

In order to take into account the fuel consumption, we consider the model proposed in [18], that is based on the results introduced in [30]. It consists of a sixth order polynomial $K(v)$ averaged over the characteristics of different cars, then suitable for a large range of vehicles:

$$\begin{aligned} K(v) = {} & 5.7 \cdot 10^{-12} \cdot v^6 - 3.6 \cdot 10^{-9} \cdot v^5 + 7.6 \cdot 10^{-7} \cdot v^4 \\ & - 6.1 \cdot 10^{-5} \cdot v^3 + 1.9 \cdot 10^{-3} \cdot v^2 + 1.6 \cdot 10^{-2} \cdot v + 0.99 \end{aligned} \tag{22}$$

where $K(v)$ is expressed in [Liters/hr] and v in [km/hr]. Differently from the exponential function used in [29], the one in (22) has a low computational burden. However, in order

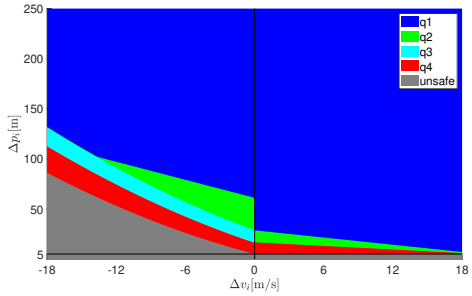

Fig. 2: Set Ω and partitions Ω_j corresponding to the leader at speed $v_{i-1} = 18$ m/s.

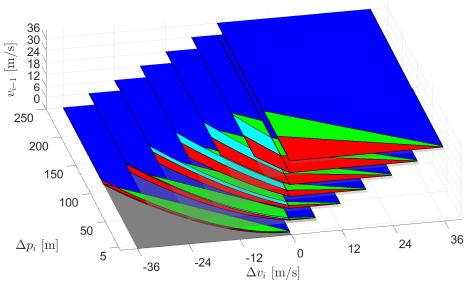

Fig. 3: 3D view of Ω and partitions Ω_j computed for different values of v_{i-1}.

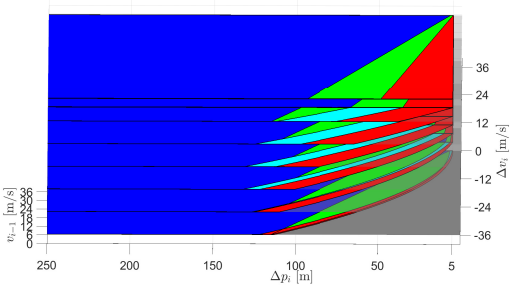

Fig. 4: 3D view of Ω and partitions Ω_j computed for different values of v_{i-1}.

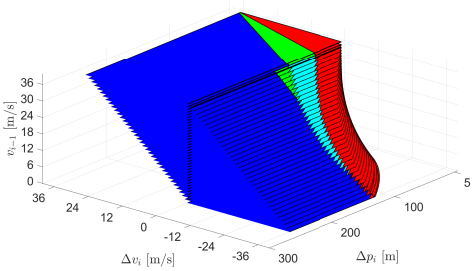

Fig. 5: Set Ω.

to evaluate the performances of the controller with respect to fuel consumption, in Section V-C we will use a more complex index proposed in [37] (see equation (39)).

B. Microscopic Optimization Problem

Let $\mathcal{N}$ be the optimization horizon with respect to which the solution of the optimization problem is computed. Given a signal x, we denote with $x(h|k)$, $h = 0, \ldots, \mathcal{N}$, the predicted value at time $k + h$ obtained by starting from the value at time k. Moreover, given a vector x and a matrix $Q \geq 0$, $\|x\|_Q = (x^T Q x)^{1/2}$ denotes the weighted Euclidean norm.

At each time k, the optimal control sequence $u_i^*(h|k)$, $h = 0, ..., \mathcal{N} - 1$, is computed according with the hybrid state $\xi_i(0|k) = \xi_i(k)$, then $u_i(k) = u_i^*(0|k)$ is applied as control input. Therefore, the same steps are repeated at time $k + 1$ when new measurements are available. We consider that each vehicle uses only local information, namely the one of the correspondent leader-follower pair. According to the meaning of each discrete state $q \in Q$, a different cost function J_q is defined so that the various objectives receive different weights, as a human driver would do. Then, according to the discrete state at time k, the cost function J_q is selected and is kept constant over the optimization horizon. Although this method leads to a sub-optimal solution, it is acceptable in a moving horizon framework. Moreover, it allows for avoiding an NP-hard problem, that would result if the state q, and consequently function J_q, are left to vary when solving the optimization problem.

To guarantee safety, the constraint

$$u_i(0|k) - a_{res}(0|k) \in [a_{\min}, a_{i-1}(k)] \tag{23}$$

is added to the optimization problem when condition

$$x_i(k) \in Dom(q_4) \ \wedge \ \Delta v_i(k) < 0 \ \wedge \ a_{i-1}(k) < 0 \tag{24}$$

is met. Then, to derive a formulation of (23) and (24) that is suitable to be included in the MPC definition, we define the parameter $\delta \in \{0, 1\}$ as

$$\delta = \begin{cases} 1 & \text{if (24) is true} \\ 0 & \text{otherwise,} \end{cases} \tag{25}$$

and (23) is rewritten as

$$u_i(0|k) - a_{res,i}(0|k) \leq a_{\max} - (a_{\max} + a_{i-1}(k))\delta. \tag{26}$$

In defining constraint (23), we consider region Ω_4 as a guard zone for continuous states that can lead to critical or emergency situations. Then, when (24) is true, the input that is going to be applied is forced to correspond to a braking action with an intensity that is greater or equal to the braking action of the vehicle ahead. As a consequence, also in the case of the worst case scenario where $\Delta p_i = \Delta E_i$ and $a_{i-1} = a_{\min}$, feasibility and collision avoidance are ensured by $u_i(0|k) - a_{res}(0|k) = a_{\min}$.

Under the assumption that the entire state x_i is measurable, we define the output vector

$$y_i = \begin{bmatrix} \Delta p_i \\ \Delta v_i \\ v_{i-1} - \Delta v_i \end{bmatrix} = \begin{bmatrix} \Delta p_i \\ \Delta v_i \\ v_i \end{bmatrix} \tag{27}$$

where the first two components are the inter-vehicular distance and speed difference, as defined for the state vector (2), and associated to the car-following situation.The third component

is the speed of the i-th vehicle. Then, we define the corresponding reference vector

$$y_i^r = [\ \Delta p_i^r\ \ \Delta v_i^r\ \ v_i^r\ ]^T, \tag{28}$$

where $(\Delta p_i^r, \Delta v_i^r) = (\Delta S(x_i), 0)$ is the reference trajectory to be tracked in a car-following situation, namely q_2, q_3, q_4. On the contrary, $v_i^r > 0$ is the reference speed for the *Free driving* situation q_1, which we assume to be a constant value. When in a car-following situation, we set the reference distance $\Delta p_i^r(h|k) = \Delta S(x_i(k)),\ \forall\, h \geq 0$, and we define $\tilde{y}_i = y_i - y_i^r$.

Given the hybrid state $\xi_i(k)$ at time k, the problem we want to solve is

$$\min_{u_i(h|k),\ h=0,\dots,\mathcal{N}-1} J_q \tag{29a}$$

s.t.

$$x_i(h+1|k) = Ax_i(h|k) + B_u u_i(h|k) + B_d a_{i-1}(h|k) + Ea_{res,i}(h|k),\ h = 0, ..., \mathcal{N}-1, \tag{29b}$$

$$x_i(0|k) = x_i(k), \tag{29c}$$

$$x_i(h|k) \in X,\ h = 0, ..., \mathcal{N} \tag{29d}$$

$$a_{i-1}(h|k) \in [a_{\min}, a_{\max}],\ h = 0, ..., \mathcal{N}-1 \tag{29e}$$

$$u_i(h|k) - a_{res,i}(h|k) \in [a_{\min}, a_{\max}],\ h = 0, ..., \mathcal{N}-1 \tag{29f}$$

$$u_i(0|k) - a_{res,i}(0|k) \leq a_{\max} - (a_{\max} + a_{i-1}(k))\delta \tag{29g}$$

where

$$J_q = \|\tilde{y}_i(\mathcal{N}|k)\|^2_{P_q} + \sum_{h=0}^{\mathcal{N}-1} \Big(\|\tilde{y}_i(h|k)\|^2_{G_q} + + \|u_i(h|k)\|^2_{R_q} + M_q c_f K_i(h|k)\tau \Big) \tag{30}$$

where $a_{res,i}(h|k) = a_{res}(x_i(h|k))$, $K_i(h|k) = K(x_i(h|k))$, c_f is the factor to convert $K_i(h|k)$ from [Liters/hr] to [Liters/s], set X as defined in (5), and δ as in (25). Although δ is an integer value, (29) is not a mixed-integer programming problem. Indeed, the value of δ depends only on the hybrid state $\xi_i(k)$ and it remains constant over all the optimization horizon, thus it is not a decision variable. Matrices $P_q, G_q \in \mathbb{R}^{3\times 3},\ P_q, G_q \geq 0$, weigh the different objectives in the cost function, and $R_q, M_q \in \mathbb{R},\ R_q, M_q \geq 0$ weigh the control effort and the consumption, respectively. $a_{i-1}(h|k)$ is the predicted acceleration of the leader vehicle, seen as a bounded disturbance. The a priori knowledge of the acceleration profile of the leader would allow a more accurate prediction and the computation of a more performing control input sequence. However, we remark that real scenarios are not fully predictable and the use of such information could still lead to non optimal solutions. According with the data available at each sampling time, we identify the following situations: 1) The follower vehicle i knows (either by measurements/estimation or V2V communication) only the current acceleration of its leader. Then, the constant speed assumption is made; 2) As in 1), the follower vehicle i knows only the current acceleration of its leader, but the constant acceleration assumption is made; 3) Each vehicle sends to the follower its own acceleration prediction, obtained by solving the optimization problem in (29) [38]. The possibility to send such information is given by V2V interconnection, and it is regulated by standards for dedicated short-range communication (DSRC) [39]. We remark that strategy 3 may suffer from unexpected events because in that case the receiving follower would compute its own control input on the basis of a wrong prediction.

We assume that each vehicle sends to the follower its acceleration forecast (case 3) by means of a Basic Safety Message (BSM, SAE J2735 [39]), thus resulting in a distributed MPC when the vehicles are in platoon formation (see [31] and [32]).

In the sequel, we explain the heuristic for the choice of the weights:

1) q_1: the follower is free to track the desired speed v^r without incurring immediate dangers, and applying fuel consumption optimization. We set $P_{q_1}(3,3), G_{q_1}(3,3) > 0$ (other elements of P_{q_1} and G_{q_1} are null) and $R_{q_1}, M_{q_1} > 0$.
2) q_2: the follower vehicle is closing in to its leader, but distance and speed are such that there is no immediate danger. The proposed cost function allows for an optimal tracking of the desired distance Δp^r considering both relative distance error and fuel consumption. We set $P_{q_2}(1,1),\ P_{q_2}(2,2),\ G_{q_2}(1,1),\ G_{q_2}(2,2) > 0$ (other elements of P_{q_2} and G_{q_2} are null) and $R_{q_2}, M_{q_2} > 0$.
3) q_3: the car-following pair is close to a risky situation. The proposed cost function allows for an optimal tracking of the desired distance Δp^r considering both the relative distance error and fuel consumption. Unlike q_2, a higher importance is given to the tracking of Δp^r with respect to the eco-driving objective. We set $P_{q_3}(1,1),\ P_{q_3}(2,2),\ G_{q_3}(1,1),\ G_{q_3}(2,2) > 0$ (other elements of P_{q_3} and G_{q_3} are null) and $R_{q_3}, M_{q_3} > 0$.
4) q_4: the distance from the previous vehicle is close to the unsafe one. The proposed cost function allows for an optimal tracking of the desired distance Δp^r considering only relative distance error, since safety has priority over fuel optimization. We set $P_{q_4}(1,1),\ P_{q_4}(2,2),\ G_{q_4}(1,1),\ G_{q_4}(2,2) > 0$ (other elements of P_{q_4} and G_{q_4} are null) and R_{q_4}, M_{q_4} to low values, or to zero.

IV. Mesoscopic Model and Optimization Problem

In this section, we discuss the introduction of traffic macroscopic data in the controller design. The purpose is to obtain a mesoscopic model for improving the overall platoon response. The possibility of exploiting macroscopic information is analysed in [12] and [14], where the authors prove that a proper definition of macroscopic variables can ensure String Stability for the platoon (see [40] for details on this topic). However, this kind of stability does not guarantee collision avoidance. Our objective is to improve the microscopic MPC-based controller defined in Section III-B, which allows addressing safety and eco-driving specifications, with the use of macroscopic variables that contain information about all the vehicles ahead. This leads to the possibility for the vehicles to anticipate any changes in the platoon state, with a consequent

harmonization of the trajectories. For control purposes, we consider the mean and variance of the microscopic quantities because of their connection with traffic macroscopic variables, as also proven by several traffic flow diagrams (see [41, ch. 4]). As a consequence, there is no need to share some microscopic information among the whole platoon, e.g., the leading vehicle acceleration or its desired speed. Then, no direct communication between the first vehicle and the others is required, except for its immediate follower [14].

A. Macroscopic Information

Given the generic vehicle $i \in \mathcal{I}_N^0$, let $\mu_{v,i}$ and $\sigma_{v,i}^2$ be, respectively, the speed mean and variance computed from vehicle 0 to vehicle i:

$$\mu_{v,i} = \frac{1}{i+1}\sum_{j=0}^{i} v_j, \quad \sigma_{v,i}^2 = \frac{1}{i+1}\sum_{j=0}^{i}(v_j - \mu_{v,i})^2. \quad (31)$$

In (31) $\mu_{v,i}$ and $\sigma_{v,i}^2$ are computed starting from the first vehicle of the platoon, but clearly, these variables could also be computed over a finite number of vehicles preceding the i-th one as in [11]. Moreover, the variables in (31) may be computed either in a distributed way by the vehicles, or by the road infrastructure that interfaces with the traffic, then can be shared either via V2V or via V2I [12]. Since we assume that the set of vehicles is homogeneous with $v_{\min} \leq v_i \leq v_{\max}$ $\forall i \in \mathcal{I}_N^0$, the maximum variance value follows from the below expression:

$$\sigma_{v,\max}^2 = \frac{(v_{\max} - v_{\min})^2}{4} = \frac{v_{\max}^2}{4}, \quad (32)$$

recalling that $v_{\min} = 0$. Then, we define the speed macroscopic function $\psi_v : \mathbb{R} \times \mathbb{R} \times \mathbb{R} \to \mathbb{R}$,

$$\psi_v(v_i, \mu_{v,i}, \sigma_{v,i}^2) = \xi_i sign(v_i - \mu_{v,i}), \quad (33)$$

where $\xi_i = 2\sqrt{\sigma_{v,i}^2}/v_{\max} \in [0,1]$, with $\xi_i = 0$ denoting the platoon being in steady-state, while $\xi_i \in (0,1]$ meaning that the string is in a transient phase. The purpose of function ψ_v in (33) is to relate the microscopic state of the i-th vehicle with that of the macroscopic traffic. Instead of considering the whole set of leader-follower vehicles pairs ahead of the i-th one, it allows for a complexity reduction of the interconnection framework without reducing the level of available information. By definition, we get $\psi_v(v_i, \mu_{v,i}, \sigma_{v,i}^2) \in [-1,1]$, where:

- $\psi_v(v_i, \mu_{v,i}, \sigma_{v,i}^2) \in [-1,0)$ identifies the case where $v_i < \mu_{v,i}$, meaning that the platoon is accelerating;
- $\psi_v(v_i, \mu_{v,i}, \sigma_{v,i}^2) \in (0,1]$ identifies the case where $v_i > \mu_{v,i}$, meaning that the platoon is decelerating;
- $\psi_v(v_i, \mu_{v,i}, \sigma_{v,i}^2) = 0$ corresponds to all vehicles having the same speed.

In order to avoid discontinuity problems due to function $sign(\cdot)$, we consider the following stable discrete-time linear system:

$$\begin{cases} \rho_i(k+1) = \lambda_\rho \rho_i(k) + \gamma \psi_v^{i-1}(k) \\ \rho_i(0) = 0 \end{cases} \quad (34)$$

where $|\lambda_\rho| < 1, \gamma > 0$ are tuning parameters that alter the filter response. The trajectory of (34) is such that $\rho_i \to 0$ as $\psi_v \to 0$. Then, it is possible to vary the filter response with respect to variations of the macroscopic variables by appropriately choosing λ_ρ and γ. The superscript $i-1$ denotes that the i-th vehicle makes use of the macroscopic information computed over the state of the vehicles ahead, up to its predecessor. For vehicle $i = 0$, we set $\psi_v^{-1} = 0$.

B. Mesoscopic Optimization Problem

As in [11], we define $\alpha = sat(1+\rho_i) \in [\alpha_{\min}, \alpha_{\max}]$ as a parameter that vary the time headways (7) defining the hybrid automaton domains:

$$\begin{aligned} &T_D'(\alpha, T_D) = \alpha T_D, \;\; T_S'(\alpha, T_S) = \alpha T_S, \\ &T_R'(\alpha, T_R) = \alpha T_R, \end{aligned} \quad (35)$$

while T_E is not modified because of the collision avoidance requirement. Analogously to the definitions in (35), we denote with $\Delta D'$, $\Delta S'$, and $\Delta R'$ the variance-based space thresholds corresponding to the definitions given in Section II-B. According to [11], the boundaries of α are chosen such that $\alpha_{\min} \in (0,1)$ and $\alpha_{\max} \in (1, 2.5)$. The effect is to enlarge, or to shrink, the regions Ω_j depending on the current traffic situation: when $\alpha \in [\alpha_{\min}, 1)$ the vehicles ahead of the i-th one are accelerating. Then, during the transient the car-following related regions shrink ($\Omega_j,\ j = 2,3,4$) and the *Free driving* one enlarges (Ω_1), such that the followers can be more reactive. When $\alpha \in (1, \alpha_{\max}]$, the vehicles ahead are decelerating, then the car-following regions enlarges, and consequently the reference distance increases letting the followers to assume a more cautious behavior. Finally, $\alpha = 1$ denotes a steady-state phase.

In addition to the new definitions of the time headways in (35), we define also a variance-based mechanism to modify the cost function weights introduced in Section III-B. The purpose is to vary the trade-off between the tracked objectives depending on the current macroscopic situation. Then, we define

$$P_q'(\alpha, G_q) = \alpha P_q, \;\; G_q'(\alpha, G_q) = \alpha G_q, \quad (36a)$$

$$R_q'(\alpha, R_q) = R_q/\alpha, \;\; M_q'(\alpha, M_q) = M_q/\alpha, \quad (36b)$$

and proper boundaries $P_q' \in [P_{\min}, P_{\max}]$, $G_q' \in [G_{\min}, G_{\max}]$, $R_q' \in [R_{\min}, R_{\max}]$, and $M_q' \in [M_{\min}, M_{\max}]$. We refer to component-wise inequalities for the matrices. Then, when the leading vehicles are accelerating, hence $\alpha < 1$, we allow for a less strict tracking of the reference distance and of the preceding vehicles speed ($P_q' < P_q$, $G_q' < G_q$), while we increase the input effort weighting ($R_q' > R_q$, $M_q' > M_q$). On the contrary, when the platoon is decelerating, $\alpha > 1$, we apply the opposite strategy.

We now define the optimization problem to be solved at each time step for the computation of the optimal control input $u_i^*(h|k)$. As in Section III-B, we consider the optimization horizon $\mathcal{N}$ and the reference vector y_i^r in (28), with $\Delta p_i^r(h|k) = \Delta S'(x_i(k))$, $\forall\, h$. Given the hybrid state (20) of the generic vehicle at time k and $\tilde{y}_i = y_i - y_i^r$, the problem to be solved is

$$\min_{u_i(h|k),\ h=0,\dots,\mathcal{N}-1} J_q' \quad (37a)$$

s.t. (29b)-(29g)

where

$$J'_q = \|\tilde{y}_i(\mathcal{N}|k)\|^2_{P'_q} + \sum_{h=0}^{\mathcal{N}-1} \Bigg(\|\tilde{y}_i(h|k)\|^2_{G'_q} + \\ + \|u_i(h|k)\|^2_{R'_q} + M'_q c_f K_i(h|k)\tau \Bigg). \quad (38)$$

As before, when in a car-following situation, we consider the i-th vehicle to receive the predicted acceleration trajectory from its predecessor. Being the mesoscopic optimization problem subject to the same constraints set as in the microscopic case, the same arguments apply for the recursive feasibility of the MPC.

TABLE I: Vehicles parameters

τ [s]	0.25	$a_{\min}$ [m/s^2]	-6
m_v [Kg]	1392.2	$a_{\max}$ [m/s^2]	6
$v_{\min}$ [m/s]	0	c_{aero} [-]	1.06
$v_{\max}$ [m/s]	36	c_{roll} [-]	0.0093

V. Simulations

In this section, we report numerical simulation obtained by the implementation of both microscopic and mesoscopic controllers that have been proposed in the previous sections, respectively (29) and (37). The simulations are performed in MATLAB&Simulink with the use of Yalmip toolbox (see [42]) for the set up and the solution of the optimization problem.

We consider a platoon of $N+1 = 11$ identical vehicles, the parameters and the desired acceleration/deceleration limits of which are reported in Table I. The horizon length is $\mathcal{N} = 10$, and the nominal weights in (30) and (38) are the following:

- $P_{q_1}(3,3) = 35$ and $P_q(1,1) = 20$, $P_q(2,2) = 35$ for $q = q_2, q_3, q_4$;
- $G_{q_1}(3,3) = 20$ and $G_q(1,1) = 6$, $G_q(2,2) = 20$ for $q = q_2, q_3, q_4$;
- $M_{q_1} = 8$, $M_{q_2} = 4$, $M_{q_3} = 2$, $M_{q_4} = 1$;
- $R_{q_1} = 14$, $R_{q_2} = 14$, $R_{q_3} = 6$, $R_{q_4} = 1$.

When the variance-based mechanism introduced in Section IV is applied, we set the following boundaries: $P'_q \in [0.75P_q, 1.25P_q]$, $G'_q \in [0.75G_q, 1.25G_q]$, $R'_q \in [0.5R_q, 1.5R_q]$, $M'_q \in [0.5M_q, 1.5M_q]$. Moreover, we set $\lambda_\rho = 0.8$ and $\gamma = 0.5$.

To validate the control strategy introduced in Section III and assess the advantages of using the macroscopic information, we test two different scenarios:

1) each vehicle in a car-following situation exploits only the trajectory forecast sent by the preceding one via BSM, then implements the microscopic controller (29) (Fig. 6);
2) the traffic macroscopic information is used along with the trajectory forecast sent via of BSM by the preceding vehicle, and the mesoscopic controller (37) is implemented (Fig. 7);

The color legend adopted is the same for all figures. Each line represents the trajectory of the variable to which the figure refers: the blue line, if present, is associated to $i = 0$, while the color scale from the light yellow to the red one is associated to the vehicles from the head to the tail of the platoon.

The simulation time is 120 seconds and is the same for all the cases considered. All vehicles have as reference speed the maximum value allowed by physical and legal limits, except the head one that tracks a piecewise reference speed as in [43]. This type of signal is used for introducing a certain level of uncertainty at the discontinuity points. Therefore, a perturbation is introduced in the system with the target to evaluate the controller robustness. We split the numerical test into three main phases:

1) $0 \leq t < 40$: at $t = 0$ the head vehicle has speed $v_0(0) = v^r = 20$ m/s, while the rest of the platoon starts with random initial conditions generated in a neighborhood of $\Delta p_i = 40$ m and v^r.
2) $40 \leq t < 80$: at $t = 40$ s the reference speed of the first vehicle changes to 10 m/s, simulating the presence of a slow speed bottleneck.
3) $80 \leq t \leq 120$ s: vehicle $i = 0$ has to reach the speed of 25 m/s, representing the return to normal traffic conditions.

A. Microscopic simulation with trajectory forecast sharing

Figures 6a, 6b and 6c show, respectively, the distance and speed trajectories, and the evolution of the discrete state. In Fig. 6b, we observe that in the first phase the vehicles are able to converge to the desired speed of $v^r = 20$ m/s after a transient characterized by the presence of limited overshoots. In the same time, they converge at a safe distance around 35 m (see Fig. 6a). In Fig. 6c, we observe that the initial perturbations affect also the evolution of the discrete states, but after few seconds of oscillations they settle to *Following* mode (q_2), that refers to a car-following situation with no immediate risk.

In the second phase, the step variation of the reference speed causes the first vehicle to make a sudden marked deceleration (see see time $40\ s$ in Fig. 6b). Since the followers base their actions upon the trajectory forecast sent with the BSM, the unexpected deceleration behaves as a disturbance that propagates through the string. In this case the information shared are not exact, causing the solution of the optimization problem computed by each vehicle to be less reliable. However, since they follow each other at a distance ΔS_i, they do not react by closely copying the behaviour of $i = 0$. As a consequence, the vehicles do not decelerate with the same intensity, with the result that the tail ones have a slower convergence to the new speed. In Fig. 6a, we observe that vehicles are able to maintain a safe distance between them; however, they get closer due to the reduction of the speed. In Fig. 6c, we observe that vehicles remain in q_2.

In the third phase, due to the new change in the reference speed, the leader is subject to a marked acceleration. In Fig. 6b, we observe that this causes the followers to initially react in an identical way; however, after few seconds the vehicles along the string reduce the intensity of their action, leading to a delayed convergence to the new reference speed. In Fig. 6c, we observe that the perturbation introduced in the system affects the discrete state evolution of $i = 1$. It reaches the *Danger* mode, meaning that it assumes a more reactive behavior in order to avoid a possible upcoming dangerous

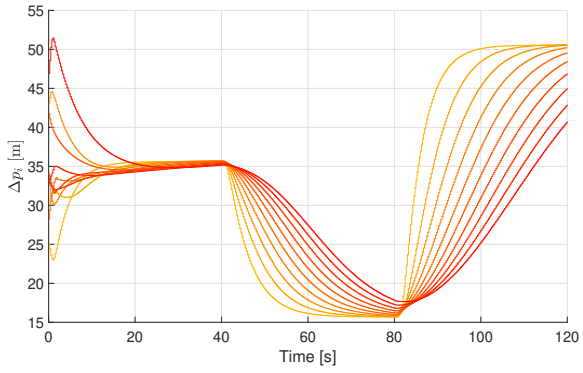

(a)

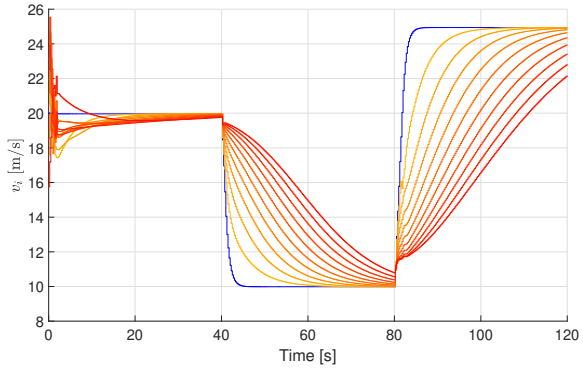

(b)

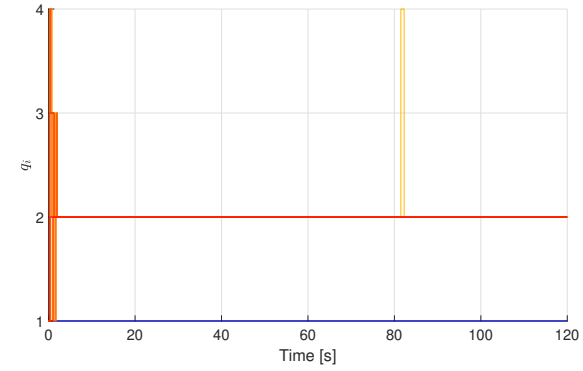

(c)

Fig. 6: First scenario: the controller exploits only the trajectory forecast contained in the BSM.

situation. Nevertheless, the platoon is able to safely manage the transient perturbations and to maintain safe inter-vehicular distances, that we see to increase as the speed increases.

B. Mesoscopic simulation with trajectory forecast sharing

In Figures 7a, 7b, 7c and 7d the numerical results obtained when the MPC based controller exploits macroscopic information, in addition to the BSM, are reported. In Fig. 7b, we note that the vehicles are able to converge at the reference speed of 20 m/s in the first phase. As in the microscopic case, this phase is characterized by perturbed initial conditions that cause oscillations during the first seconds of simulation. In Fig. 7d the macroscopic variable α is able to capture the presence of these perturbations. Then, this information is translated

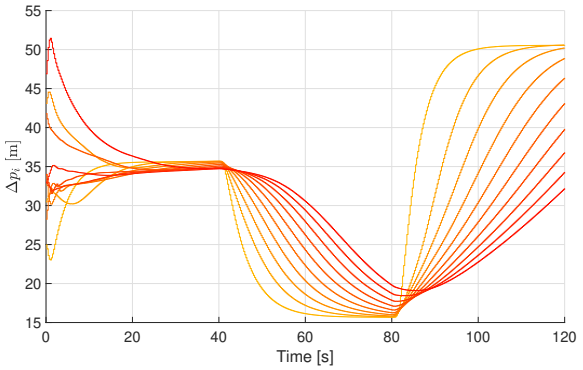

(a)

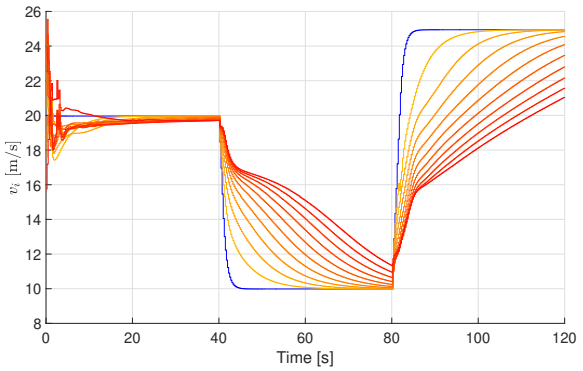

(b)

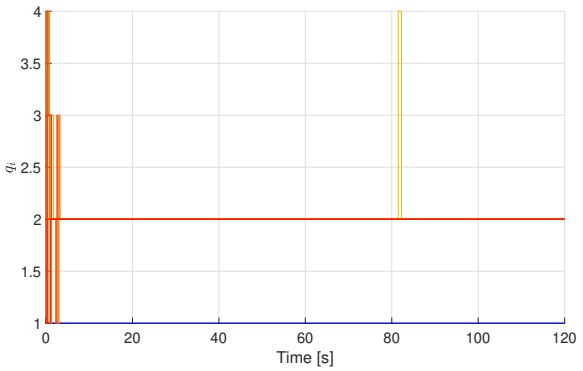

(c)

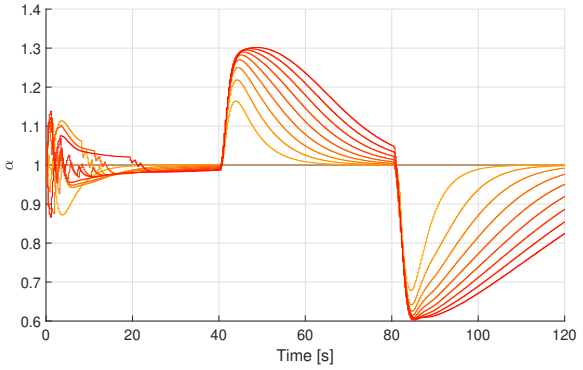

(d)

Fig. 7: Second scenario: the controller exploits the trajectory forecast in the BSM and the macroscopic information.

into the reference distance definition ($\Delta S_i'$), causing the inter-vehicular distances to show a slower convergence rate than the microscopic case. Similarly to the first scenario, the discrete states settle to the *Following* mode, or q_2 (Fig. 7a).

In the second phase, the step variation of the reference speed introduces a perturbation that propagates through the string. In Fig. 7b, we observe that the use of macroscopic information, in the form of speed mean and variance, helps the vehicles to dampen the perturbation faster than in the microscopic scenario. Thanks to the macroscopic variable, information about the marked deceleration fast propagates towards the tail vehicles. The effects of the macroscopic variable α on the platoon can be mainly observed on the speed trajectories evolution: the tail vehicles are able to anticipate their deceleration, remaining at a greater distance with respect to the microscopic case (see Fig. 7a). The same fast response is seen in the third phase. In this case, vehicles anticipate their action by appropriately scaling the velocity along the platoon. In Fig. 7c, the discrete states show the same behaviour as in the microscopic scenario. However, since the macroscopic information is used to vary the reference distance $\Delta S_i'$, we observe the inter-vehicular distance trajectories to have a slower convergence rate than the microscopic case.

Fig. 7d reports the evolution of the macroscopic variable α. We observe that it captures the state of the platoon, in particular when the high step variation of the reference speed is commanded. Its increasing magnitude lets the tail vehicles to notice that the ahead ones are in a transient phase; while its value being lower than 1, or vice versa, gives information about what type of transient phase is occurring, i.e., the acceleration or the deceleration respectively. We remark here that at each sampling time the current value of the macroscopic variable is held constant when mesoscopic optimization problem (37) is solved. In this regard, our future work will focus on the possibility to predict the evolution of α with respect to the traffic state.

C. Comments on simulations

As shown by the numerical results in Figures 6 and 7, the proposed MPC-based algorithms determine proper control actions that ensure safety of the entire platoon. The use of BSM for sharing trajectories forecast allows reducing the inaccuracy about the future evolution of the preceding vehicle, except when an unexpected situation occurs (e.g., a non predicted speed variation). When something unpredictable happens, the BSM propagates inaccurate information, so that a perturbation is propagated. In such cases, the problem of String Instability may arise (see [40]), because the platoon could amplify the magnitude of the perturbations as they flow towards the tail vehicles. In both scenarios presented here, the controllers are able to handle this situation so that this phenomenon does not occur. However, enriching the control action with macroscopic information helps to improve the platoon response. Indeed, the tail vehicles show anticipatory behaviour when the reference speed value varies.

In order to better appreciate the performances of the proposed control algorithms, we compare the results of the mesoscopic approach with respect to a microscopic setting where the consumption term is neglected, i.e., $M_q = 0$ for each $q \in \{1, 2, 3, 4\}$, simulated under the same conditions described at the beginning of Section V. We provide a comparison in terms of energy consumption per unit mass by computing for each vehicle the quantity

$$W_i = \int_0^{t_f} v_i(\tilde{t})(u_i(\tilde{t}) + a_{res}(\tilde{t}))d\tilde{t}, \tag{39}$$

where $t_f = 120$ s, $u_i = F_{T,i}/m_v$, and $a_{res} = F_{res}/m_v$ (see [37]). We compare the consumption of the leader vehicle (which is not affected by the macroscopic behaviour of the platoon, and for this reason not taken into account for the energy computation since it always has the same information scenario), with the rest of the platoon. Then, we obtain for the set of follower vehicles the following results: i) microscopic case with no fuel consumption optimization: the set of follower vehicles saves 14.7042%; ii) microscopic case with fuel consumption: the set of follower vehicles saves 15.2981%; iii) mesoscopic case with fuel consumption: the set of follower vehicles saves 15.0652%. As it is possible to see, both the mesoscopic and the microscopic controllers with fuel consumption optimisation perform better than the microscopic controller without fuel consumption optimisation. More specifically, there is a gain of 4% and 2%, respectively. The mesoscopic case is shown to lose performance with respect to the microscopic one; this again confirms the anticipative behaviour due to the utilisation of macroscopic information, which also takes place during the acceleration phase. Consequently, faster accelerations lead to higher consumption, which is the price to pay for having more fluid platoons in acceleration mode. However, we expect this behaviour to be compensated in a mixed situation of several braking and acceleration phases. For the sake of clarity, the simulations consider only a short time evolution to give the reader a clear understanding and comparison of controllers' performance in the considered cases. In fact, the presented simulations allow the appreciation of both the human-based MPC strategy performance and the improvements due to the utilisation of macroscopic information, but the examined time and space are too small for providing validation. On the basis of the obtained results showing the efficacy of the proposed control approaches, the analysis of more complex scenarios will be part of future work.

VI. Conclusions

A human-inspired ACC based on MPC and capable to exploit macroscopic information is presented. In order to include human characteristics in the control development, first a human-inspired microscopic hybrid automaton is considered. Then, a microscopic optimization problem targeting collision avoidance (safety) and consumption minimization (eco-driving) is defined, where a different cost function for each discrete state of the hybrid automaton is suggested. The vehicles are supposed to be equipped with V2X communication technology, enabling each leader to share his near future predicted trajectory with the follower. Then, we extended the microscopic framework by considering macroscopic information of the traffic flow, thus deriving a mesoscopic

controller. To test the robustness of the proposed approach, two different scenarios were simulated: the first scenario refers to the microscopic case, where each follower use only the trajectory prediction sent by its leader; in the second scenario, each vehicle implements the mesoscopic controller. The results show that the proposed controllers are always able to ensure the safety of the vehicles and that the use of macroscopic variables allows each vehicle to anticipate the needed control actions.

Future work will focus on the robustness analysis against external disturbances as well as the presence of communication and actuation delays. Also, more complex traffic scenarios will be analysed as well as methodologies for traffic evolution prediction. Furthermore, quantifying the optimal macroscopic information will be worth future investigation.

REFERENCES

[1] Z. Wang, G. Wu, and M. J. Barth, "Cooperative eco-driving at signalized intersections in a partially connected and automated vehicle environment," IEEE Transactions on Intelligent Transportation Systems, vol. 21, no. 5, pp. 2029–2038, 2020.

[2] R. E. Stern, S. Cui, M. L. Delle Monache, R. Bhadani, M. Bunting, M. Churchill, N. Hamilton, R. Haulcy, H. Pohlmann, F. Wu, B. Piccoli, B. Seibold, J. Sprinkle, and D. B. Work, "Dissipation of stop-and-go waves via control of autonomous vehicles: Field experiments," Transportation Research Part C: Emerging Technologies, vol. 89, pp. 205 – 221, 2018.

[3] B. Othman, G. De Nunzio, A. Sciarretta, D. Di Domenico, and C. Canudas-de Wit, Connectivity and Automation as Enablers for Energy-Efficient Driving and Road Traffic Management, pp. 1–40. New York, NY: Springer New York, 2020.

[4] P. Caravani, E. De Santis, F. Graziosi, and E. Panizzi, "Communication control and driving assistance to a platoon of vehicles in heavy traffic and scarce visibility," IEEE Transactions on Intelligent Transportation Systems, vol. 7, pp. 448–460, Dec 2006.

[5] S. W. Loke, "Cooperative automated vehicles: A review of opportunities and challenges in socially intelligent vehicles beyond networking," IEEE Transactions on Intelligent Vehicles, vol. 4, no. 4, pp. 509–518, 2019.

[6] E. Uhlemann, "The US and Europe Advances V2V Deployment [Connected Vehicles]," IEEE Vehicular Technology Magazine, vol. 12, pp. 18–22, June 2017.

[7] C. Badue, R. Guidolini, R. V. Carneiro, P. Azevedo, V. B. Cardoso, A. Forechi, L. Jesus, R. Berriel, T. M. Paixão, F. Mutz, L. de Paula Veronese, T. Oliveira-Santos, and A. F. De Souza, "Self-driving cars: A survey," Expert Systems with Applications, vol. 165, p. 113816, 2021.

[8] S. Lefèvre, A. Carvalho, and F. Borrelli, "A learning-based framework for velocity control in autonomous driving," IEEE Transactions on Automation Science and Engineering, vol. 13, pp. 32–42, Jan 2016.

[9] C. Lv, X. Hu, A. Sangiovanni-Vincentelli, Y. Li, C. M. Martinez, and D. Cao, "Driving-style-based codesign optimization of an automated electric vehicle: A cyber-physical system approach," IEEE Transactions on Industrial Electronics, vol. 66, pp. 2965–2975, April 2019.

[10] A. Iovine, F. Valentini, E. De Santis, M. D. Di Benedetto, and M. Pratesi, "Safe human-inspired mesoscopic hybrid automaton for longitudinal vehicle control," IFAC-PapersOnLine, vol. 48, no. 27, pp. 155 – 160, 2015. Analysis and Design of Hybrid Systems ADHS.

[11] A. Iovine, F. Valentini, E. De Santis, M. D. Di Benedetto, and M. Pratesi, "Safe human-inspired mesoscopic hybrid automaton for autonomous vehicles," Nonlinear Analysis: Hybrid Systems, vol. 25, pp. 192 – 210, 2017.

[12] M. Mirabilio, A. Iovine, E. De Santis, M. D. Di Benedetto, and G. Pola, "String stability of a vehicular platoon with the use of macroscopic information," IEEE Transactions on Intelligent Transportation Systems, vol. 22, no. 9, pp. 5861–5873, 2021.

[13] I. Karafyllis, D. Theodosis, and M. Papageorgiou, "Nonlinear adaptive cruise control of vehicular platoons," International Journal of Control, vol. 0, no. 0, pp. 1–23, 2021.

[14] M. Mirabilio, A. Iovine, E. De Santis, M. D. Di Benedetto, and G. Pola, "Mesoscopic controller for string stability of platoons with disturbances," IEEE Transactions on Control of Network Systems, vol. 9, no. 4, pp. 1754–1766, 2022.

[15] C. Pasquale, S. Sacone, S. Siri, and A. Ferrara, "A new Micro-Macro METANET model for platoon control in freeway traffic networks," in 2018 21st International Conference on Intelligent Transportation Systems (ITSC), pp. 1481–1486, Nov 2018.

[16] D. Swaroop and R. Huandra, "Intelligent cruise control system design based on a traffic flow specification," Vehicle System Dynamics: International Journal of Vehicle Mechanics and Mobility, vol. 30, pp. 319–344, November 1998.

[17] A. Ibrahim, M. Čičić, D. Goswami, T. Basten, and K. Johansson, "Control of platooned vehicles in presence of traffic shock waves," IEEE Intelligent Transportation Systems Conference (ITSC), pp. 1727–1734, 2019.

[18] G. Piacentini, P. Goatin, and A. Ferrara, "Traffic control via platoons of intelligent vehicles for saving fuel consumption in freeway systems," IEEE Control Systems Letters, vol. 5, no. 2, pp. 593–598, 2021.

[19] J. Lygeros, K. H. Johansson, S. N. Simic, J. Zhang, and S. S. Sastry, "Dynamical properties of hybrid automata," IEEE Transactions on Automatic Control, vol. 48, pp. 2–17, Jan 2003.

[20] P. Nilsson, O. Hussien, A. Balkan, Y. Chen, A. D. Ames, J. W. Grizzle, N. Ozay, H. Peng, and P. Tabuada, "Correct-by-construction adaptive cruise control: Two approaches," IEEE Transactions on Control Systems Technology, vol. 24, pp. 1294–1307, July 2016.

[21] R. Wiedemann and U. Reiter, "Microscopic traffic simulation: the simulation system mission," Background and Actual State, Project ICARUS (V10552), Final Report. Brussels: CEC., 1992.

[22] H. Fritzsche, "A model for traffic simulation," Traffic Engineering and Control, vol. 35, no. 5, pp. 317–321, 1994.

[23] S. Lin, B. De Schutter, Y. Xi, and H. Hellendoorn, "Integrated urban traffic control for the reduction of travel delays and emissions," IEEE Transactions on Intelligent Transportation Systems, vol. 14, pp. 1609–1619, Dec 2013.

[24] A. Sciarretta and A. Vahidi, Energy-Efficient Speed Profiles (Eco-Driving), pp. 131–178. Cham: Springer International Publishing, 2020.

[25] P. Liu, U. Ozguner, and Y. Zhang, "Distributed mpc for cooperative highway driving and energy-economy validation via microscopic simulations," Transportation Research Part C: Emerging Technologies, vol. 77, pp. 80–95, 2017.

[26] S. W. Smith, Y. Kim, J. Guanetti, R. Li, R. Firoozi, B. Wootton, A. A. Kurzhanskiy, F. Borrelli, R. Horowitz, and M. Arcak, "Improving urban traffic throughput with vehicle platooning: Theory and experiments," IEEE Access, vol. 8, pp. 141208–141223, 2020.

[27] Y. Hu, C. Chen, J. He, and B. Yang, "Eco-platooning for cooperative automated vehicles under mixed traffic flow," IEEE Transactions on Intelligent Transportation Systems, vol. 22, no. 4, pp. 2023–2034, 2021.

[28] M. Yu and J. Long, "An eco-driving strategy for partially connected automated vehicles at a signalized intersection," IEEE Transactions on Intelligent Transportation Systems, vol. 23, no. 9, pp. 15780–15793, 2022.

[29] M. Mirabilio, A. Iovine, E. De Santis, M. D. Di Benedetto, and G. Pola, "A microscopic human-inspired adaptive cruise control for eco-driving," in 2020 European Control Conference (ECC),

pp. 1808–1813, 2020.
[30] K. Ahn, H. Rakha, A. Trani, and M. Van Aerde, "Estimating vehicle fuel consumption and emissions based on instantaneous speed and acceleration levels," Journal of transportation engineering, vol. 128, no. 2, pp. 182–190, 2002.
[31] W. B. Dunbar and D. S. Caveney, "Distributed receding horizon control of vehicle platoons: Stability and string stability," IEEE Transactions on Automatic Control, vol. 57, no. 3, pp. 620–633, 2012.
[32] Y. Zheng, S. Ebel Li, K. Li, F. Borrelli, and J. Hedrick, "Distributed model predictive control for heterogeneous vehicle platoons under unidirectional topologies," IEEE Transactions on Control Systems Technology, vol. 25, pp. 899–910, May 2017.
[33] J. Guanetti, Y. Kim, and F. Borrelli, "Control of connected and automated vehicles: State of the art and future challenges," Annual Reviews in Control, vol. 45, pp. 18 – 40, 2018.
[34] Z. Wang, Y. Bian, S. E. Shladover, G. Wu, S. E. Li, and M. J. Barth, "A survey on cooperative longitudinal motion control of multiple connected and automated vehicles," IEEE Intelligent Transportation Systems Magazine, vol. 12, no. 1, pp. 4–24, 2020.
[35] L. Guzzella and A. Sciarretta, Vehicle Energy and Fuel Consumption – Basic Concepts, pp. 13–46. Berlin, Heidelberg: Springer Berlin Heidelberg, 2013.
[36] Q. Luo, A.-T. Nguyen, J. Fleming, and H. Zhang, "Unknown input observer based approach for distributed tube-based model predictive control of heterogeneous vehicle platoons," IEEE Transactions on Vehicular Technology, vol. 70, no. 4, pp. 2930–2944, 2021.
[37] C. R. He, J. I. Ge, and G. Orosz, "Fuel efficient connected cruise control for heavy-duty trucks in real traffic," IEEE Transactions on Control Systems Technology, vol. 28, no. 6, pp. 2474–2481, 2020.
[38] Y. Kim, J. Guanetti, and F. Borrelli, "Robust eco adaptive cruise control for cooperative vehicles," in 2019 18th European Control Conference (ECC), pp. 1214–1219, June 2019.
[39] J. Kenney, "Dedicated short-range communications (dsrc) standards in the united states," Proceedings of the IEEE, vol. 99, pp. 1162–1182, July 2011.
[40] S. Feng, Y. Zhang, S. E. Li, Z. Cao, H. X. Liu, and L. Li, "String stability for vehicular platoon control: Definitions and analysis methods," Annual Reviews in Control, vol. 47, pp. 81–97, March 2019.
[41] M. Treiber and A. Kesting, Traffic flows dynamics. Springer, 2013.
[42] J. Löfberg, "Automatic robust convex programming," Optimization methods and software, vol. 27, no. 1, pp. 115–129, 2012.
[43] G. Gunter, D. Gloudemans, M. L. Delle Monache, et al., "Are commercially implemented adaptive cruise control systems string stable?," IEEE Transactions on Intelligent Transportation Systems, vol. 22, no. 11, pp. 6992–7003, 2021.

Marco Mirabilio received the B.Sc. and M.Sc. degrees in Computer and Systems Engineering from the University of L'Aquila, L'Aquila, Italy, in 2015 and 2018, respectively and the European Doctorate degree in Systems and Control Theory in 2022 from the University of L'Aquila, L'Aquila, Italy. His research interests include modeling, simulation, and control of autonomous vehicles, developing novel strategies able to exploit the information sharing among the whole traffic. He is now employed as Control System Engineer for diesel thermal engine control development for low-emission targets.

Alessio Iovine (M'18) received the B.Sc. and M.Sc. degrees in electrical engineering and computer science from the University of L'Aquila, L'Aquila, Italy, in 2010 and 2012, respectively, and the European Doctorate degree in information science and engineering in 2016 from the University of L'Aquila, L'Aquila, Italy, in collaboration with CentraleSupélec, Paris-Saclay University, Paris, France. From 2016 to 2020, he held Post-Doctoral positions at University of L'Aquila, Efficacity Research Center (France), University of California at Berkeley (USA), and CentraleSupélec.

From 2020, he is a Researcher at CNRS and a member of L2S, CentraleSupélec, Paris-Saclay University. His research interests are related on advanced control methods for power and energy systems and traffic control, with smartgrids, integration of renewables and storage devices, autonomous vehicles and cooperative intelligent transportation systems as core applications.

Elena De Santis received the degree in Electrical Engineering (cum laude) from the University of L'Aquila, L'Aquila, Italy, in 1983. Since 1998 she is teaching Optimal Control in the same University, as Associate Professor, and from 2019 as Full Professor. Her research interests are cyber physical systems, discrete event systems and ICT for environmental sustainability.

Maria Domenica Di Benedetto is a Professor of Automatic Control at University of L'Aquila (Italy). She received her Master degree in Electrical Engineering and Computer Science from University of Roma "La Sapienza" and holds the PhD degree ("Docteur-Ingenieur" Spécialité Automatique et Traitement du Signal) and the degree "Doctorat d'Etat ès Sciences" (Spécialité Sciences Physiques), both from Université de Paris-Sud (Orsay, France). She is an IEEE and IFAC Fellow. Her research interests are in the areas of nonlinear and hybrid systems control theory, diagnosability and predictability in cyber-physical systems, and applications to traffic control, smart grids and biological systems.

Giordano Pola (M'07–SM'15) received the "Laurea Degree" in Electrical Engineering in July 2000 and the Ph.D. degree in Electrical Engineering and Computer Science in June 2004, from the University of L'Aquila, Italy. From 2018 at present he is an Associate Professor at the University of L'Aquila, Italy. His research interests include modeling, analysis and control of hybrid, embedded, networked and distributed systems.